

# Hardware Digital Color Enhancement for Color Vision Deficiencies

Yu-Chieh Chen and Tai-Shan Liao

**Up to 10% of the global population suffers from color vision deficiency (CVD) [1], especially deuteranomaly and protanomaly, the conditions in which it is difficult to discriminate between red and green hues.<sup>1)</sup> For those who suffer from CVD, their career fields are restricted, and their childhood education is frustrating. There are many optical eye glasses on the market to compensate for this disability. However, although they are attractive due to their light weight, wearing these glasses will decrease visual brightness and cause problems at night. Therefore, this paper presents a supplementary device that comprises a head-mounted display and an image sensor. With the aid of the image processing technique of digital color space adjustment implemented in a high-speed field-programmable gate array device, the users can enjoy enhanced vision through the display without any decrease in brightness.**

**Keywords: FPGA, color vision deficiencies, HMD.**

## I. Introduction

Different kinds of inherited color deficiencies result from partial loss of function in one or more different cone photo-receptors in the retina. The most frequent human color vision deficiencies involve insensitivity to the middle or long wavelength in the human cone systems. A person with this deficiency has difficulty discriminating reds, yellows, and greens from one another. Other color deficiencies, such as discriminating blues from yellows, are very rare. The rarest condition involves complete color blindness, monochromacy, in which one cannot distinguish any color from gray.

There are many eyeglasses on the market designed to address these conditions. Although the glasses are light-weight and require no batteries, people wearing them will suffer from loss of brightness in their vision, which greatly decreases night vision. Therefore, many research groups have used digital imaging for color compensation. Yang proposed a method to adapt colors based on visual content for people with color vision deficiency [2]. Cheng proposed a re-coloring algorithm to enhance the accessibility of the re-coloring image for people with color vision deficiency [3]. Ohkubo used a PC-based color-compensation vision system for color-blind people [4]. That system transfers confused colors to distinguishable colors, and therefore can help color-blind people recognize traffic signals.

In this paper, we use an FPGA as the system device controller, which consists of a complementary metal oxide semiconductor (CMOS) image sensor that senses the image and a liquid crystal on silicon (LCOS) display device which displays an enhanced image. The LCOS has high resolution and low-power consumption benefits, making it well-suited to micro-projections and head-mounted display devices.

---

Manuscript received Jan. 26, 2010; revised Aug. 16, 2010; accepted Aug. 30, 2010.

Yu-Chieh Chen (phone: +886 3 5779911 ext. 572, email: bjamesch@itrc.narl.org.tw) is with the Instrument Technology Research Center, National Applied Research Laboratories, Hsinchu, Taiwan, and is also with the Department of Electrical Engineering, National Tsing-Hua University, Hsinchu, Taiwan.

Tai-Shan Liao (email: tsliao@itrc.narl.org.tw) is with the Instrument Technology Research Center, National Applied Research Laboratories, Hsinchu, Taiwan.  
doi:10.4218/etrij.11.1510.0009

<sup>1)</sup> CVD is quite common. In Europe, 8% of European males and .5% of European females suffer from this problem, while among Pingalese islanders, 5% to 10% of the population have CVD.

Therefore, there are many head-mounted display products made from LCOS panels in the consumer market, such as MYVU [5] and MicroVision [6].

## II. Design Methodology

This section first introduces color space and color deficiency and then defines a saturation parameter ( $\Delta s$ ) for enhancing the digital image. Through several degrees of enhanced  $\Delta s$ , we find that when  $\Delta s=+20$  the enhanced image can have relatively similar color compared to the original color.

### 1. Color Space

Color is composed of many different wavelengths of light. Figure 1 shows the visible spectrum. An object which reflects uniformly across the entire spectrum is called white. On the contrary, an object that reflects nothing is called black. In this way, if a specific part of the spectrum reflects much more than the others, we can see that specific light. For example, if the object reflects the spectrum located in the range of 600 nm to 700 nm, we would define the light as being red.

The purpose of a color space is to facilitate the specification of colors using some standard, generally accepted way. In essence, a color model is a coordinate system and a subspace within that system in which each color is represented by a single point. Most color space systems used today are oriented toward hardware or applications using color monitors and a broad class of color video cameras; for example, RGB (red, green, blue) spaces for monitor displaying, CMYK (cyan, magenta, yellow, black) spaces for color printing, and HSI (hue, saturation, intensity) spaces, which correspond more closely to the way humans describe and interpret color [7].

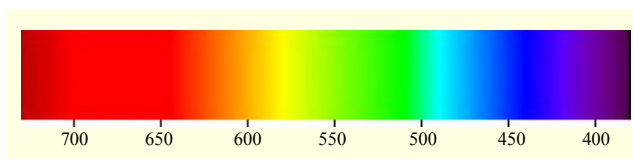


Fig. 1. Visible spectrum on nanometer scale.

### 2. Color Vision Deficiencies

There are three types of cone-shaped cell in the human retina, each containing a different pigment, which are activated when the pigments absorb light. The absorption spectra for these cone types differ. One is maximally sensitive to short wavelengths, one to medium wavelengths, and one to long wavelengths, and their peak sensitivities are in the blue, yellowish-green, and yellow regions of the spectrum,

Table 1. Simulated vision for anomalous trichromats.

Normal vision	Protanomaly
Tritanomaly	Deuteranomaly

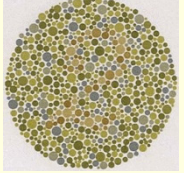
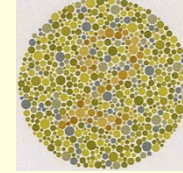
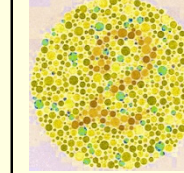
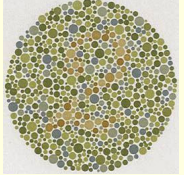
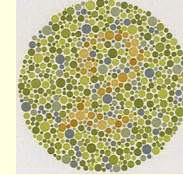
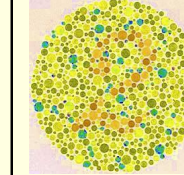
respectively. The absorption spectra of all three systems cover almost all visible spectra. The sensitivity of normal color vision actually depends on the overlap between the absorption spectra of these three cones. The different colors are recognized when the different cone types are stimulated to different extents. Red light, for example, stimulates the long wavelength cones much more than the other two. Reducing the wavelength causes the other two cone systems to be increasingly stimulated, causing a gradual change in hue. Many of the genes involved in color vision are on the X chromosome, making color blindness more common in males than in females.

Due to the different sensitivity of the photoreceptors in each person's retina, the human eye may perceive a completely different color although the color stimulus from an object is the same. Those people with protanomaly (anomalous red cones), deuteranomaly (anomalous green cones), or tritanomaly (anomalous blue cones) are called anomalous trichromats. In order to distinguish red or green, protanomalous observers need stronger red light intensity than a normal observer, and deuteranomalous observers need stronger green light intensity than a normal observer. Table 1 shows simulated images [8] to illustrate normal vision, protanomaly, tritanomaly, and deuteranomaly. Since one tenth of the population suffers from protanomaly and deuteranomaly, we focus on enhancing the image for protanomaly and deuteranomaly in this paper.

### 3. Color Enhancement Method

In the HSI color space, hue defines the specific color, and saturation defines the purity of the color in the range of [0, 1]. Since protanomaly and deuteranomaly cause trouble in distinguishing red and green, we strengthen the saturation parameter in HSI color spaces to enhance the purity of the color.

**Table 2.** Simulated vision of enhanced digital image as seen by a person with protanomaly and deuteranomaly.

Simulation of digital enhanced image as seen by protanope.		
		
$\Delta s = -20$	$\Delta s = +20$	$\Delta s = +100$
Simulation of digital enhanced image as seen by deuteranope.		
		
$\Delta s = -20$	$\Delta s = +20$	$\Delta s = +100$

Let  $\Delta s$  be the saturation enhancing value,  $S$  is the original saturation value, and  $eR$ ,  $eG$ ,  $eB$  are the enhanced RGB values in a pixel. The modified HSI to RGB equations are shown as

$$eR(\Delta s) = I \left[ 1 + \frac{(S + \Delta s) \cos H}{\cos(60^\circ - H)} \right], \quad (1)$$

$$eG(\Delta s) = 1 - (eR + eB), \quad (2)$$

$$eB(\Delta s) = I [1 - (S + \Delta s)]. \quad (3)$$

Table 2 illustrates the simulation of the enhanced digital image with different values of  $\Delta s$ , which will be observed by someone having protanomaly or deuteranomaly. The value of mean error  $\Delta e$  (the range of five pixels in a set) is defined in (4), which is the difference between the original image and the enhanced image when a protanope or deuteranope watches the image. The  $\Delta R$ ,  $\Delta G$ , and  $\Delta B$  in (5) to (7) are the mean differences of RGB colors in a pixel set between the original image and the enhanced image viewed by a protanope or deuteranope:

$$\Delta e = \left| \text{mean}(R, G, B) - \text{mean}(eR, eG, eB) \right|, \quad (4)$$

$$\Delta R = \left| \text{mean}(R) - \text{mean}(eR) \right|, \quad (5)$$

$$\Delta G = \left| \text{mean}(G) - \text{mean}(eG) \right|, \quad (6)$$

$$\Delta B = \left| \text{mean}(B) - \text{mean}(eB) \right|. \quad (7)$$

Figure 2 shows the  $\Delta e$  curve versus the  $\Delta s$  curve based on

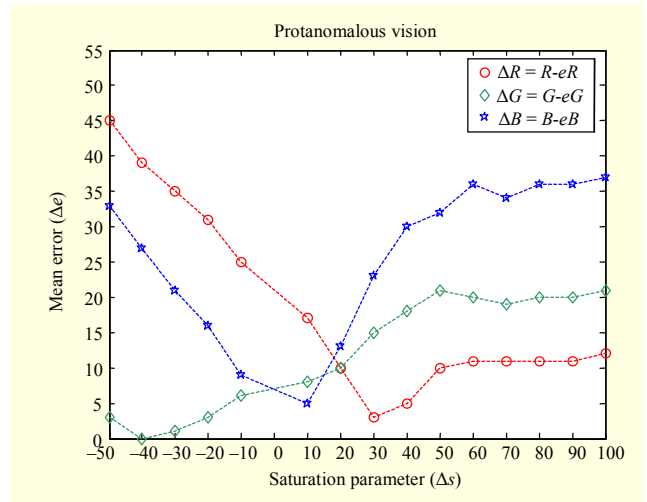


**Fig. 2.**  $\Delta e$  curve versus  $\Delta s$  curve based on protanomalous vision.

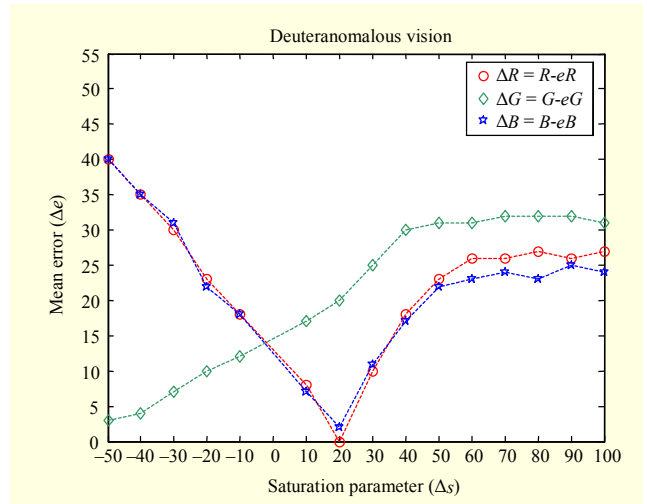


**Fig. 3.**  $\Delta e$  curve versus  $\Delta s$  curve based on deuteranomalous vision.

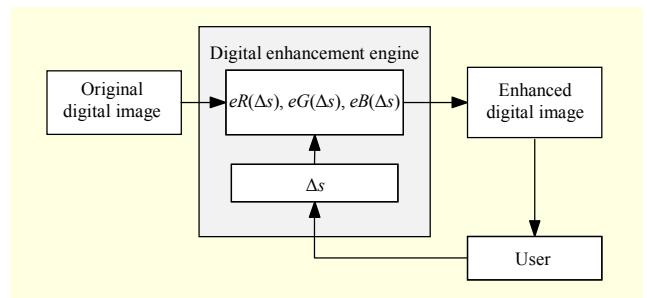


**Fig. 4.** Color enhancement method.

protanomalous vision, and Fig. 3 shows the  $\Delta e$  curve versus the  $\Delta s$  curve based on deuteranomalous vision. When  $\Delta s$  is +20, both protanomalous vision and deuteranomalous vision have a relatively small  $\Delta e$  value. Therefore, we assume that we can get an enhanced image by setting a  $\Delta s$  value to meet the

requirements of both protanomalous and deuteranomalous users.

As shown in Fig. 4, the original digital image is delivered from the image sensor to the digital enhancement engine (DEE). The DEE enhanced the original digital image based on the adjustment of the  $\Delta s$  value which is fed-back from the user. Finally, the user can achieve the enhanced digital image which is closer to the original image observed by a normal person.

### III. System Structure

As shown in Fig. 5, the proposed device consists of six individual function blocks: the image sensing unit, Bayer color space to RGB conversion unit, DEE, LVDS signal generating unit, and LCOS display unit. Because this device is wearable, the features of a long battery life, light weight, compactness, and low-power consumption are required. We used Verilog [9], a hardware description language, to implement different function blocks in a FPGA as a single-chip solution. By taking advantage of the FPGA's parallel computation power, image processing can exceed real-time vision requirements by about 30 fps at a resolution of 640×480 pixels. A suitable FPGA chosen for this device is critical. A high gate count will increase power consumption, while having too few gates will not satisfy the design requirements. The proposed device uses a Cyclone III FPGA made by Altera [10] as the core unit. Table 3 shows the specification of this FPGA, which integrates the Bayer color space to RGB converting unit, the DEE, and the LVDS signal generator. The image sensor is a MT9M011 sensor from Micron, and the LCOS display device is from Himax [11].

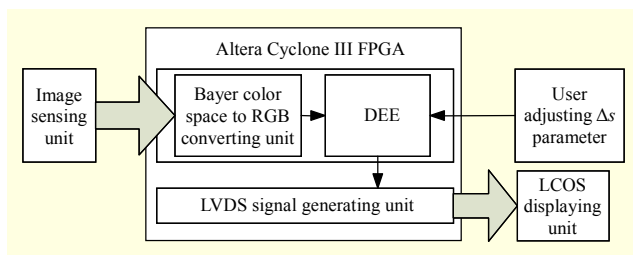


Fig. 5. System structure of supplementary device for color deficiencies.

Table 3. Specifications of Altera Cyclone III EP3C5 FPGA.

Parameter	Value
Usable logic gates	5,136
RAM (kb)	414
Multiplexers	23
PLLs	2

### 1. Image Sensing Unit

The experimental design in this study uses an MT9M011 CMOS sensor, and the maximum image resolution is 1280×1024 pixels. This sensor incorporates sophisticated camera functions on-chip, such as gamma compensation, windowing, column and row skip mode, and snapshot mode. This sensor is programmable through a simple two-wire serial interface and consumes little power. An on-chip analog-to-digital converter provides a 10-bit per pixel resolution. Both VSYNC and HSYNC signals are output on dedicated pins, along with a pixel clock that is synchronized with valid image data. Table 4 lists the key performance parameters of the MT9M011 CMOS sensor. To simplify the converter design, we only read the eight most significant bits of each pixel from the image sensing unit into the Bayer color space to the RGB converting unit in the FPGA for further image processing.

Table 4. Key performance parameters of MT9M011 CMOS image sensor.

Parameter	Typical value
Optical format	1/3 inch (5:4)
Active image size	4.6 mm (H) × 3.7 mm (V)
Active pixels	1,280 (H) × 1,024 (V) pixels
Pixel size	3.6 μm × 3.6 μm
Master clock	25 MPS / 25 MHz
ADC resolution	10-bit, on-chip
Power consumption	129 mW (full resolution) 70 mW (preview mode)

### 2. Bayer Color Space to RGB Conversion Unit

In general, a display unit can only decode RGB 24-bit color space which has 24 data bits in each pixel: 8 bits in red, 8 bits in green, and 8 bits in blue. Unfortunately, the image sensor outputs Bayer color space image data which cannot be directly used in this type of display unit. Therefore, we implement a simplified Bayer-to-RGB interpolation method to convert the Bayer color image data to RGB color space image data [12]-[14]. Figure 6 depicts the Bayer color image array, which is translated by a gamma compensator before the data is sent out from the CMOS image sensor. We defined four pixels as a single processing unit, as shown in Fig. 7, for the image interpolation process. The processing unit contains two green pixels in both  $reg(x, y)$  and  $reg(x+1, y+1)$ , a red pixel in  $reg(x+1, y)$ , and a blue pixel in  $reg(x, y+1)$ , where  $(x, y) \in I$ . Let  $P_n(R, G, B)$  be the RGB 24-bit image data in each RGB color space pixel. Each  $P_n(R, G, B)$  in a operating unit can be defined as

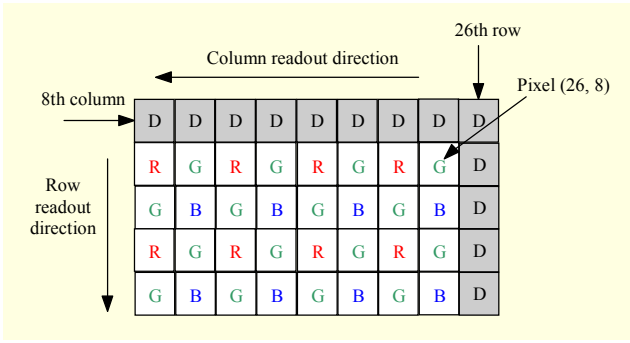


Fig. 6. Bayer color space image which is sent out from MT9M011 CMOS image sensor unit.

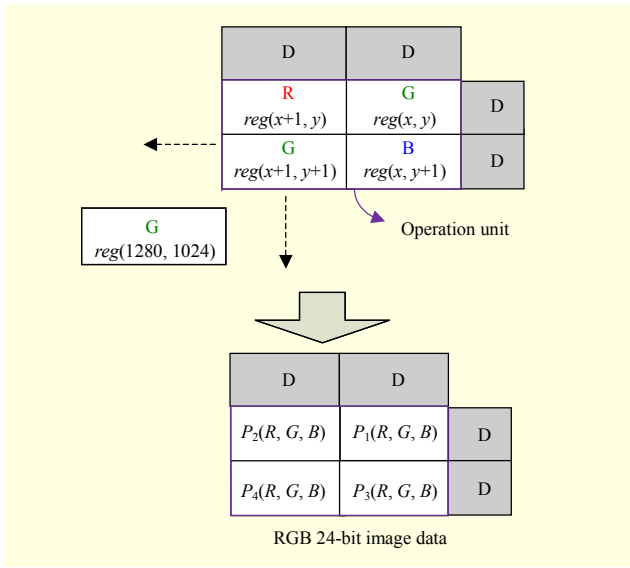


Fig. 7. Processing of Bayer color image data to RGB 24-bit image data.

$$P_{1-3}(R, G, B) = [reg(x+1, y), reg(x, y), reg(x, y+1)], \quad (8)$$

$$P_4(R, G, B) = [reg(x+1, y), reg(x+1, y+1), reg(x, y+1)]. \quad (9)$$

Finally, we use (8) and (9) to determine all the remaining unknown *RGB* information for other pixels in a frame image.

### 3. Digital Enhancement Engine

As we can see in Figs. 3 and 4, protanomalous vision and deuteranomalous vision have relatively small  $\Delta e$  values when  $\Delta s$  is +20. However, the user may need different  $\Delta s$  value according to his or her individual and personal condition. To simplify the algorithm for ease of implementation in the DEE, we multiply an empirical parameter of 1.2 to the original red value as in (10). Then, we modify (1) to (3) and obtain the corresponding equations which are (10) to (12):

$$eR(\Delta s) = 1.2 * R, \quad (10)$$

$$eG(\Delta s) = 1 - (eR + eB), \quad (11)$$

$$eB(\Delta s) = \left[ \frac{1}{3} (R + B + G) \right] * [1 - eS]. \quad (12)$$

The image from CMOS image sensor can be transferred to an enhanced image for the CVD by using (10) to (12) in the DEE. Finally, the enhanced image is sent to the LCOS display unit for the user.

### 4. LVDS Digital Generating Unit

In the high-speed signal transmission field, the ratio between the transit state and stable state is close to 1. Therefore, it becomes more and more difficult to transfer high-speed signals. The LVDS signal format is designed for the transmission of high-speed signals. An LVDS signal is formed by a pair of differential signals. The two identical signals have a 180 degree phase shift, as Fig. 8 shows. Equations (13) to (16) indicate the relationship of each voltage level:

$$V_{icm} = \frac{1}{2} (V_1 + V_2), \quad (13)$$

$$V_{id} = V_1 - V_2, \quad (14)$$

$$V_1 = V_{icm} + \frac{V_{id}}{2}, \quad (15)$$

$$V_2 = V_{icm} - \frac{V_{id}}{2}. \quad (16)$$

Figure 9 shows the surrounding circuit of the LVDS signal pin from the FPGA device. Because  $V_{id}$  and  $V_{icm}$  are formed by the subtraction of two signals, noise can be eliminated. The

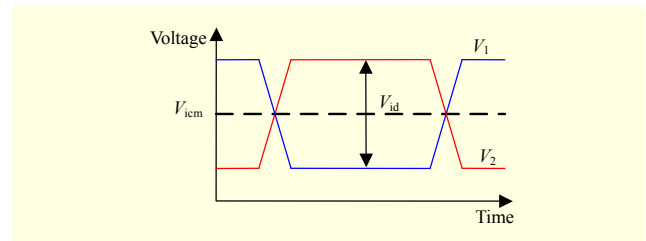


Fig. 8. LVDS signal.

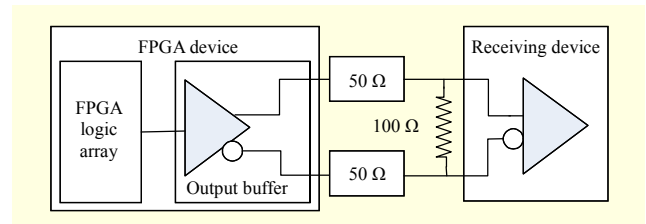


Fig. 9. Surrounding circuit of LVDS signal generator.

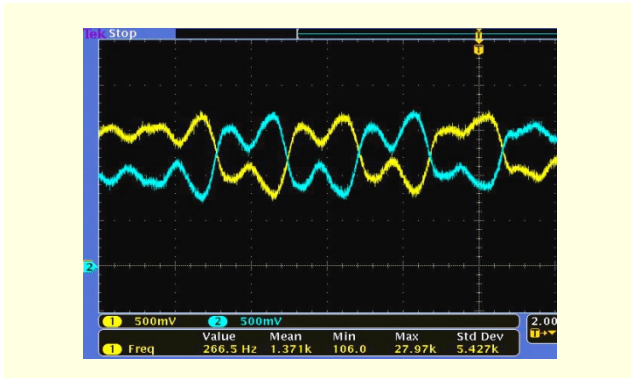


Fig. 10. Using FPGA to generate 350 MHz LVDS signal.

device is designed based on space limitations and cost concerns. Since the LCOS receives the LVDS signal format, the LVDS signal generator is implemented in FPGA. Therefore, the image signal is sent directly from the FPGA to the LCOS display device. Figure 10 shows the LVDS image signal sent from the FPGA with a voltage level of 500 mV for each signal. The LCOS display unit requires a 50 MHz pixel clock and 8-bit parallel image data. Because the LVDS signal transfers image data serially, it must scale up the frequencies from 50 MHz parallel data to 350 MHz serial data.

### 5. Image Display Unit

LCOS panel technology was developed in 1997. LCOS structure is similar to an LCD but has a smaller pixel size and is better suited to head-mounted displays. Figure 11 shows the LCOS display module HX7007A, which supports a 640×480 pixel resolution of RGB 24-bit color and requires a 50 MHz clock rate to perform the analog to digital conversion in the panel. The module consists of a white LED for the light source, a zoom lens which magnifies the image, and a beam splitter to display the enhanced image in front of the human eyes.

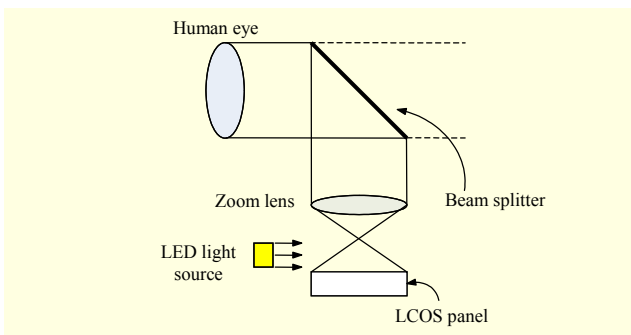


Fig. 11. LCOS image display module.

## IV. Experiment

The hardware-based digital image enhancing device for

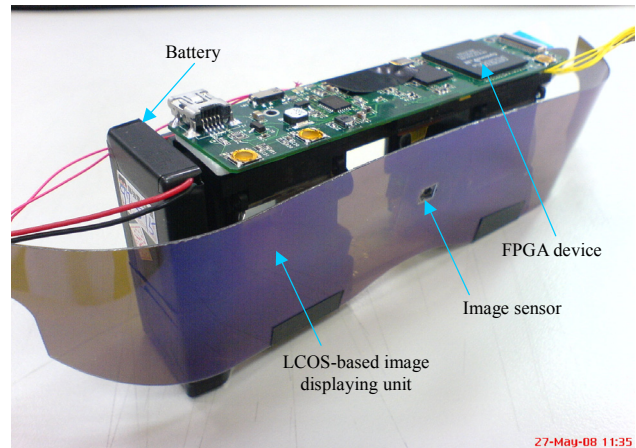


Fig. 12. Hardware-based image enhancing device.

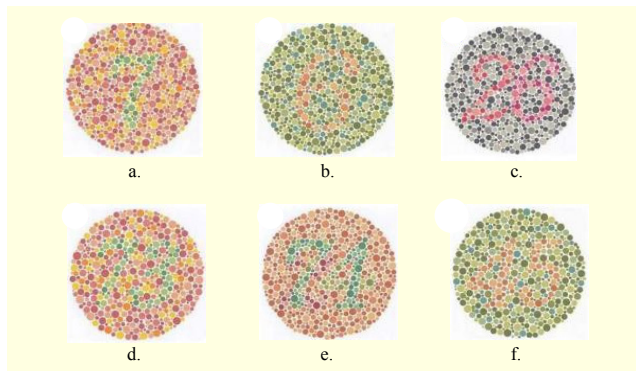


Fig. 13. Colorblind testing card array.

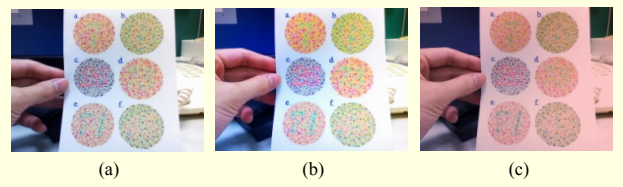


Fig. 14. (a) Original image captured from CMOS image sensor, (b) digitally-enhanced image which captured from CMOS image sensor, and (c) simulation image of an optically-enhanced image for protanomaly.

CVD is shown in Fig. 12. In experiments, we use a color-blind testing card array to test how the user would see the digitally-enhanced image and the optically-enhanced image. We repeated the above procedures using six different colorblind testing patterns as shown in Fig. 13. Figure 14 shows the image captured from the CMOS sensor. We first calculate each  $\Delta R$ ,  $\Delta G$ , and  $\Delta B$  values of different colorblind test patterns for both the digitally-enhanced technique and optically-enhanced technique. Then we plot the  $\Delta(RGB)$  curve, which is defined as  $\Delta(RGB) = \text{mean}[\Delta R, \Delta G, \Delta B]$ . We can see in Fig. 15 that almost all of the digitally-enhanced images have lower  $\Delta RGB$

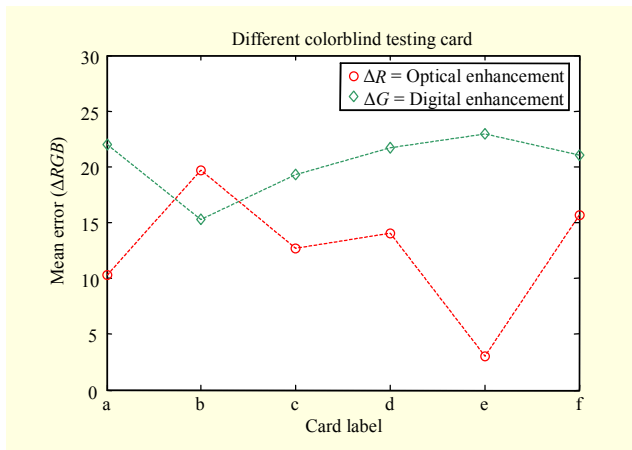


Fig. 15. Curve of  $\Delta RGB$  numbers versus different colorblind testing patterns observed by a protanope.

numbers than the  $\Delta RGB$  numbers of those which are optically enhanced. Only one label marked as “b” in the horizontal axis has the opposite result. This may be caused when the pixel color, which has been chosen to calculate the  $\Delta RGB$  number in a pixel set in the optically-enhanced image, has a better result than the pixel color chosen in the digitally-enhanced image. However, based on the experiment, the images enhanced by digital means still have a better result than those enhanced optically.

## V. Conclusion

This paper presents a hardware method for compensating images for CVD. The device is composed of a digital image from a CMOS image sensor and a set of LCOS image display devices to implement color enhancement to help those with CVD. By adjusting one saturation parameter  $\Delta s$ , the enhanced digital image can reduce the effects of protanomaly and deuteranomaly, while the optical enhancement method can only reduce the effects of either protanomaly or deuteranomaly in separate devices. Using an FPGA as the main processing unit, the enhanced image can be displayed in real time. Moreover, implementing different function blocks in an FPGA device can reduce the components of the system device and its power consumption. In the future, this device can help colorblind people recognize color by adding the visual contents adaptation function in the device to help with everyday activities such as reading traffic lights.

## References

- [1] Genetics Home Reference: <http://ghr.nlm.nih.gov/condition/color-vision-deficiency>
- [2] S. Yang and Y.M. Ro, “Visual Contents Adaption for Color

Vision Deficiency,” *Image Process. Conf.*, vol. 1, Sept. 2003, pp. 453-456.

- [3] T.C. Jen et al., “Image Recolorization for the Colorblind,” *Acoustics, Speech, Signal Process. Conf.*, Apr. 2009, pp. 1161-1164.
- [4] T. Ohkubo and K. Kobayashi, “A Color Compensation Vision System for Color-blind People,” *SICE*, Aug. 2008, pp. 1286-1289.
- [5] MYUV, 2007. <http://www.myvu.com/>
- [6] Microvision, 2007. [http://www.microvision.com/wearable\\_displays](http://www.microvision.com/wearable_displays)
- [7] C. Gonzalez and E. Woods, *Digital Image Processing*, 2nd ed., Prentice Hall Publishers, 2002, pp. 289-290.
- [8] H. Brettel, F. Vienot, and J.D. Mollon, “Computerized Simulation of Color Appearance for Dichromats,” *J. Optical Society America*, vol. 10, no. 10, Oct. 1997, pp. 2647-2655.
- [9] E. Thomas and R. Moorby, *The Verilog Hardware Description Language*, 5th ed., Kluwer Academic Publishers, 2002.
- [10] Altera, 2007. EP3C5F256C8N, <http://www.altera.com>
- [11] Himax, 2006. <http://www.himaxdisplay.com/en/product/7007le.htm>
- [12] J.M. Perez, P. Sanchez, and M. Martinez, “Low-Cost Bayer to RGB Bilinear Interpolation with Hardware-Aware Median Filter,” *ICECS*, Dec. 2009, pp. 916-919.
- [13] K. Nallaperumal et al., “A Novel Adaptive Weighted Color Interpolation Algorithm for Single Sensor Digital Camera Images,” *Computational Intell. Multimedia Appl.*, Dec. 2007, pp. 477-481.
- [14] Y.C. Chen and T.S. Liao, “Converter Translates Bayer Raw Data to RGB Format,” *EDN*, Feb. 2010, pp. 47-48.



**Yu-Chieh Chen** received the BS in mechanical engineering from Yunlin University of Science and Technology, Yunlin, Taiwan, in 2002, and the MS in mechanical and electro-mechanical engineering from Tamkang University, Taipei, Taiwan, in 2005. He is an associate researcher at the Instrument Technology Research Center, National Applied Research Laboratories. He is currently working toward his PhD at Tsing-Hua University, Hsinchu, in the Neuro-Engineering Laboratory. He also is an associate researcher at the Instrument Technology Research Center, National Applied Research Laboratories. His research interests include low-power analog and mixed-signal VLSI for biomedical applications and control theory.



**Tai-Shan Liao** received his PhD in electronic engineering from Chung Yuan Christian University in 2003. He is currently a researcher at Instrument Technology Research Center, National Applied Research Laboratories.